Run-to-Tumble Variability Controls the Surface Residence Times of E. coli Bacteria

Gaspard Junot, Thierry Darnige, Anke Lindner, Vincent Martinez, Jochen Arlt, Angela Dawson, Wilson C. K. Poon, Harold Auradou, Eric Clément

Run-to-Tumble Variability Controls the Surface Residence Times of *E. coli* Bacteria

Gaspard Junot,[1] Thierry Darnige,[1] Anke Lindner,[1] Vincent A. Martinez,[3] Jochen Arlt,[3] Angela Dawson,[3] Wilson C. K. Poon,[3] Harold Auradou,[2] and Eric Clément[4,1]

[1]*PMMH, UMR 7636 CNRS, ESPCI Paris, PSL Research University, Sorbonne Université and Université Paris Cité, 7-9 quai Saint-Bernard, Paris, 75005, France*

[2]*Université Paris-Saclay, CNRS, FAST, 91405 Orsay, France*

[3]*SUPA and the School of Physics and Astronomy, The University of Edinburgh, Peter Guthrie Tait Road, Edinburgh EH9 3FD, United Kingdom*

[4]*Institut Universitaire de France (IUF)*

(Received 20 July 2021; accepted 19 April 2022; published 14 June 2022)

Motile bacteria are known to accumulate at surfaces, eventually leading to changes in bacterial motility and biofilm formation. We use a novel two-color, three-dimensional Lagrangian tracking technique to follow simultaneously the body and the flagella of a wild-type *Escherichia coli*. We observe long surface residence times and surface escape corresponding mostly to immediately antecedent tumbling. A motility model accounting for a large behavioral variability in run-time duration reproduces all experimental findings and gives new insights into surface trapping efficiency.

DOI: 10.1103/PhysRevLett.128.248101

Suspensions of active particles such as motile microorganisms display rich, often counterintuitive, phenomena unseen in suspensions of passive colloids [1], such as an effective viscosity lower than the pure solvent [2,3], the formation of "living crystals" [4], or accumulation at the walls [5–7]. Persistence in the swimming direction along surfaces is a generic contributing to "surface trapping" along with hydrodynamic [5] or eventually transient adhesion [8]. Bacterial surface motility is involved in many industrial, biomedical, or environmental issues, such as bacterial contamination or biofouling [9,10]. Attachment of bacteria to surfaces often leads to the buildup of hard-to-eradicate biofilms and is problematic for medical implants [11], water purification systems [12], and many industrial processes [13]. In nature, the attachment of bacteria to plant roots constitutes the first physical step in many plant-microbe interactions [14]. Adhesion may originate from surface restriction to flagellar motion [15] and trigger the secretion of polysaccharides for structuring mature biofilms [16]. The initial stage preceding surface adhesion is therefore the "residence time" τ of the swimming bacterium at the surface. This quantity is key to understanding and modeling the problems of bacterial contamination in environmental or biomedical situations [17,18]. Wild-type (WT) *Escherichia coli* perform run and tumble (RT), in which straight runs are interspersed with tumbles where the swimming direction changes rapidly. The escape mechanism of those bacteria is still not fully understood [19,20]. To date, the detailed microhydrodynamics of this phenomenon remains challenging even for state-of-the-art numerics [21]. Recent experiments using digital holographic microscopy to capture 3D trajectories of wild-type *E. coli* [22] near a solid surface suggested that surfaces inhibit tumbling and polarize the posttumbling direction parallel to the surface, so that tumbling is not a particularly effective escaping mechanism.

In our study, individual motile *E. coli* bacteria were tracked using two-color three-dimensional tracking (2*C*3DT) that provides visualization of the flagella dynamics with an unprecedented precision. Observations of displacements close to a surface were made during long periods of time allowing, for the first time, the assessment of the surface residence time distribution, the angular distributions for arrival and escape, and the distribution of duration of unbundling events. Those distributions were compared with measurements performed away from the surface. We find long surface residence times and demonstrate that tumbling is the dominant escape mechanism. To reproduce our observations, we adapted and simulated a recent "behavioral variability" (BV) model [23] in which the run-to-tumble transition displays a much larger variability compared with a Poisson probability distribution of transition [24].

Methods.—We implemented 2*C*3DT by combining Lagrangian 3D tracking [23,25] with two-color fluorescence imaging [26] [see Fig. 1(a)] on an inverted epifluorescence microscope (Zeiss-Observer, Z1, C-Apochromat $63\times/1.2$ W objective). To avoid signal overlap and emission leakage, we engineered an *E. coli* strain (AD62) with body and flagella fluorescence in the green and red respectively (see the Supplemental Material [27]). A two-color LED light source (Zeiss Colibri 7) and a dichroic image splitter (Hamamatsu) are used to project two monochrome images onto two different regions of the

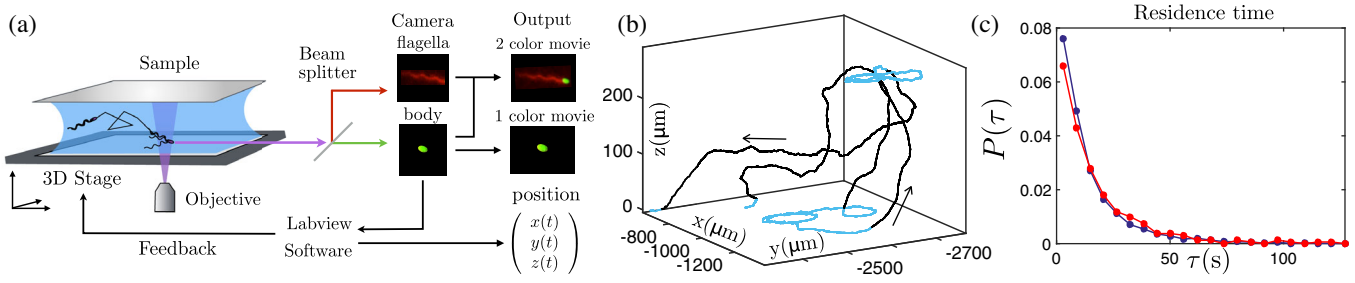

FIG. 1. (a) Sketch of the Lagrangian tracking giving the position of the bacterium and videos in one or two colors. (b) 3D view of a bacterium trajectory, parts of the trajectory below 8 μm from the surface are in blue; arrows indicate the trajectory direction. (c) Distribution $P(\tau)$ of residence times τ at the surface. Experimental data are in red and simulations in blue.

camera chip. Computer-controlled movement of the microscope stage keeps the body of a selected bacterium in focus [25], and images (1024×1024 pixels) are recorded at 80 frames/ sec with a Hamamatsu ORCAFlash 4.0, C11440 camera. Green and red images are then superimposed to create a movie of the tracked bacterium and its flagella bundle (see video in the Supplemental Material [27]). Photobleaching limits flagella imaging to a minute, and thus, long-time behavior cannot be observed with this technique. For long-time tracking, we use a strain with nonfluorescent flagella (RP437) that allows one-color recording of 66 independent cells over 7 h, with the longest track being of $\gtrsim$20 min duration. Bacteria were grown and prepared using standard protocols [26] (see the Supplemental Material [27]). For imaging, a 80 μL drop with $\lesssim 3 \times 10^7$ cells mL^{-1} was placed between two glass plates separated by 260 μm and sealed.

Experimental results.—To measure the surface residence time τ [see Fig. 1(b)], we need to identify when a cell arrives and escapes from a surface. A bacterium is considered in the bulk when the body centroid is at a distance from the nearest surface $\Delta z > \delta = 8$ μm (a typical cell body + flagella length) and arrived at a surface when $\Delta z < 3$ μm. The "surface region" is left again when, subsequently, $\Delta z > \delta$. The residence time τ is then the interval between the first and last time a bacterium crosses $\Delta z = 3$ μm and is not influenced by small variations in the choice of these two lengths (see the Supplemental Material [27]). The measured distribution of surface residence times $P(\tau)$ [see Fig. 1(c)] has mean $\langle\tau\rangle = 21$ s and a long tail extending to a maximum observed τ of 373 s $\lesssim 20\tau$. The long-tailed, highly nonexponential nature of $P(\tau)$ is emphasized when plotted against $\ln\tau$ [Fig. 2(a)] and fitted to a log-normal distribution. These residence times are very long as compared to the—usually reported—average run time of WT *E. coli* ($\sim$1 s according to Ref. [34]). So, a bacterium seems to tumble many times during its residence at a surface before escaping, apparently confirming the suggestion that tumbling would be an inefficient escape mechanism [22]. For this track series, we also measured the incoming and escape angles for cells arriving (θ_{in}) and leaving (θ_{out}) the surface region, defined as $\theta_{\text{in,out}} = \arcsin(\mathbf{p}_{\text{in,out}} \cdot \mathbf{n})$ where $\mathbf{p}_{\text{in,out}}$ is a unit vector aligned with the body of the bacterium and $\mathbf{n}$ a unit vector normal to the surface. The probability distributions [Figs. 2(b)–(c)] are obtained from 366 pieces of bacterial tracks reaching or leaving the surface. First, to understand the incoming angle distribution, one can assume a random swimming orientation in the bulk, yielding a probability to have a swimming direction between θ and $\theta + d\theta$, proportional to $d[\sin(\theta)] = \cos(\theta)d\theta$. For a given time interval, the number of bacteria actually counted, crossing the surface at a distance δ and heading toward the wall, is $\propto V_B \sin(\theta)$ (V_B being the bacterial velocity). Therefore,

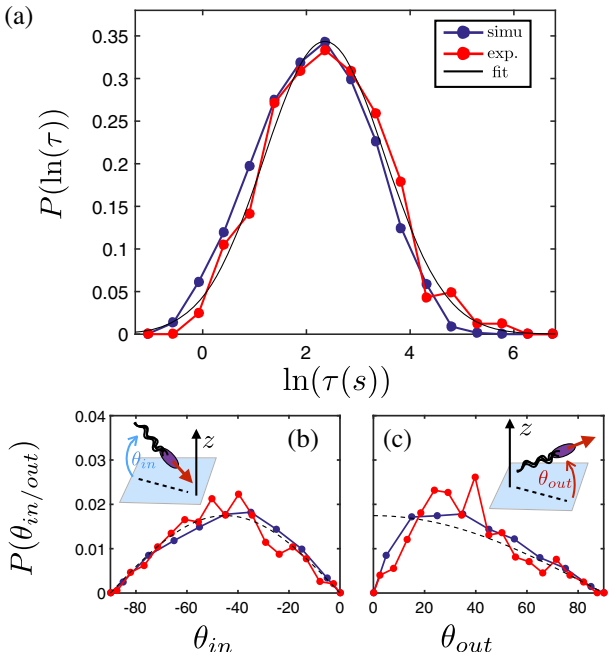

FIG. 2. Comparison between experiment (in red) and simulations (in blue). (a) Distribution of the logarithm of the residence time ($\langle\ln(\tau)\rangle = 2.39$ and $\sigma = 1.12$). Experimental data correspond to Fig. 1(c); the black line is a Gaussian fit ($\langle\ln(\tau)\rangle = 2.36$ and $\sigma = 1.16$). (b),(c) Distributions of the incoming and escape angles from "single-color" tracking. The black dashed line is the distribution $P(\theta_{\text{in}}) = -(\pi/180)\sin(\theta_{\text{in}})\cos(\theta_{\text{in}})$ in (b) and $P(\theta_{\text{out}}) = (\pi/180)\cos(\theta_{\text{out}})$ in (c).

after normalization, the probability density to observe bacteria crossing a distance δ with an angle θ_{in} is expected to be $P(\theta_{\text{in}}) = -(\pi/180)\sin\theta_{\text{in}}\cos\theta_{\text{in}}$, which agrees with the experimental results [see Fig. 2(b)]. Now, to understand $P(\theta_{\text{out}})$, let us consider the case of a bacterium at a surface with an orientation pointing toward the bulk. If the bacterium does not tumble before reaching the boundary $\Delta z = \delta$, it will cross this height. We then expect $P(\theta_{\text{out}}) = (\pi/180)\cos\theta_{\text{out}}$. Comparing this expression with the experimental data [Fig. 2(c)], one can see a dip around $\theta_{\text{out}} = 0$ and also a peak around 30°. The deficit in the probably density originates from the fact that a cell leaving at a grazing angle ($\theta_{\text{out}} \to 0$) needs to swim straight for long times before reaching $\Delta z = \delta$, hence maximizing its chances for another tumbling event *en route*. Either this will reorient the cell back to the surface (failed escape), or the bacterium will be logged at $\Delta z = \delta$, as having escaped at a different (likely higher) angle.

Next, we characterize the tumbling statistics using 2*C*3DT image sequences to identify unambiguously what we call the "unbundling phase," where at least one flagellum is observed outside the flagella bundle. Importantly, the "unbundling phase" as defined here does not necessarily mean continuous and uninterrupted changes of direction as already noticed by Turner *et al.* [20]. These unbundling events are then different from tumbles based on changes of orientation [34,35] or on velocity distributions [36]. In the Supplemental Material [27], for completeness, we discuss this point extensively. However here, the purpose is to compare characteristic features of the tumbling process in the bulk and at the surface directly issued from the observed flagellar dynamics. Figure 3(a) shows the trajectory of a typical cell swimming at the surface before escaping. We manually identify the beginning and the end of the flagella unbundling process by replaying relevant sequences of the two-color movie back and forth. A time lapse of a typical unbundling event is shown in Fig. 3(b) (see the video in the Supplemental Material [27]). From such analysis, we obtain $P(\tau_{\text{un}})$, the probability distributions of the bulk and near-wall unbundling phase duration, displayed in Fig. 3(c) (τ_{un} is compiled from 119 and 241 events respectively). The two distributions collapse indicating that the surface does not affect the tumbling statistics as visualized on the unbundling events: in each case, $P(\tau_{\text{un}})$ is peaked around $\tau_{\text{un}} = 0.34$ s with a mean $\langle\tau_{\text{un}}\rangle \approx (0.8 \pm 0.1)$ s. We determine experimentally that only a fraction of τ_{un} leads to a reorientation and that this fraction can be taken as random within τ_{un} (see the Supplemental Material [27]). This would then yield a mean reorientation time of about 0.4 s, a value significantly larger than the mean tumbling times previously reported (around 0.1 s [34–36]). Although tumble events do not always lead to an escape [Fig. 3(a)], escape is tightly coupled to tumble. The time interval histogram between an escape event and the previous tumble event is narrowly peaked around zero

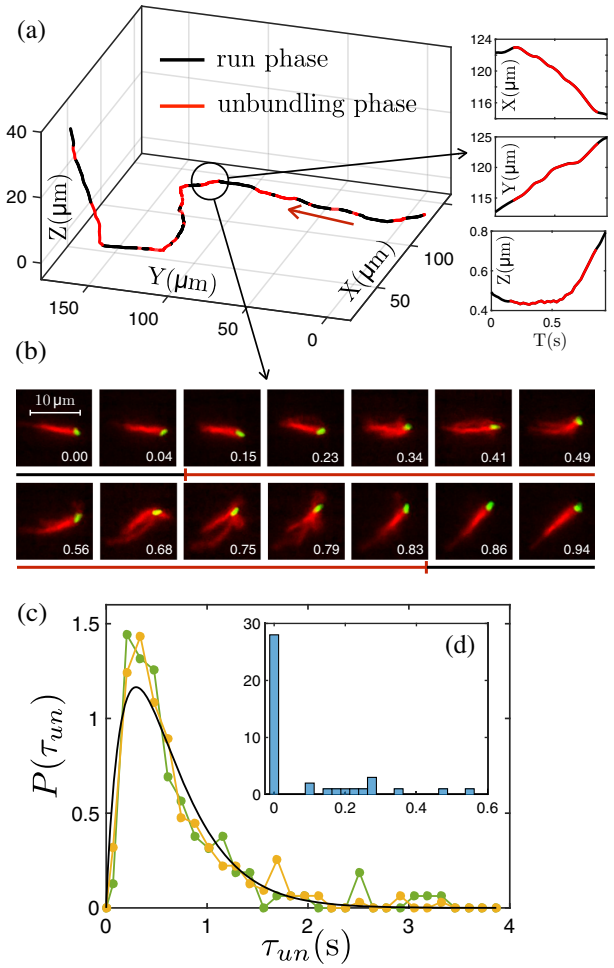

FIG. 3. (a) 3D trajectory and $x(t)$, $y(t)$, $z(t)$ coordinates of a bacterium (AD62) near the surface. Red parts show unbundling events and the arrow the trajectory direction. (b) Time lapse of an unbundling event; each image is an overlay of three consecutive frames. The color of the line indicates when the unbundling event starts and ends; the total duration is 0.71 s. (c) Distribution of the unbundled time τ_{un} at surfaces (orange) and in the bulk (green). The black line is a fit using a gamma distribution of parameter $(k, \theta) = (1.9, 0.33\text{ s})$. (d) Histogram of time τ_d between an escape event and the closest previous unbundling event.

[see inset of Fig. 3(d)], i.e., almost every escape is immediately preceded by a tumble. In contrast, a smooth-swimmer strain (CR20) with suppressed tumbling shows residence times longer than our mean observation time of 374 s (see the Supplemental Material [27]). Therefore, tumbling is indeed the dominant escape mechanism for a surface-trapped WT *E. coli* cell.

Model and computer simulations.—To understand our experimental findings, we simulate bacterial trajectories using the BV model and parameters taken from Ref. [23] to describe the RT statistics. This model accounts for an inherent stochasticity due to the concentration fluctuations of a phosphorylated protein, CheY-P, promoting the switching from counterclockwise to clockwise of the flagella

motor rotation and initiating the tumbling process [24,37]. In the model, the internal parameter δX represents fluctuations in the CheY-P concentration around the mean, normalized by the standard deviation. Its dynamics is modeled by a Ornstein-Uhlenbeck process leading to a tumbling event rate scaling as $\exp[\Delta_n \delta X]$, where parameter Δ_n is rendering the sensitivity of the run-to-tumble transition to CheY-P concentration (see model details and parameter choices in the Supplemental Material [27]). We call this internal time-resolved variable $\delta X(t)$ the swimmer "mood" since for low values, a bacterium will likely run for a long time and explore large distances whereas for larger values it would rather tumble and locally forage.

To model the surfaces, we purposely reduce the complexity of steric hindrance, hydrodynamics, and other interactions between a bacterium and a surface [5–7,38] to simple alignment rules. A particle arriving from the bulk and reaching a surface ($\Delta z = 0$) is immediately aligned with it. After tumbling, if the orientation points toward the wall, the cell is realigned with the surface keeping $\Delta z = 0$. Otherwise, it leaves the surface with this new orientation. Trajectories simulated using the BV model show a residence time distribution that matches experiments [Fig. 2(a)] without any fitting parameter. However, modeling the run-time distribution as the uncorrelated Poisson process with an average run time ≈1 s [24] does not reproduce the observed $P(\tau)$ as shown in the Supplemental Material [27]. The residence time is then the consequence of the large distribution of run times. The simulated distributions of θ_{in} and θ_{out} also match the experimental observations [see Figs. 2(b) and 2(c)]. For θ_{in}, in spite of a tiny but visible deviation with the numerical results, probably rooted in finite confinement effects, one can conclude as Molaie *et al.* [39] did, that the cell incoming angle is essentially reflecting a random swimming orientation. For θ_{out}, the small-angle "dip" in $P(\theta_{\text{out}})$ is reproduced. To estimate the extent of this depletion, note that if a bacterium does not reach the escape limit $\Delta z = \delta$ before the mean run time $\langle \tau_r \rangle$ (= 2.32 s in our model), it will likely tumble. The angle corresponding to a traveling time of $\langle \tau_r \rangle$ over a distance δ at average speed $\bar{v} = 26\ \mu$m/s is $(\delta/\bar{v}\langle \tau_r \rangle) \approx 7.6°$. We therefore expect depletion in $P(\theta_{\text{out}})$ at angles $\lesssim 10°$, as observed. Note, however, that we do not reproduce numerically the small peak in $P(\theta_{\text{out}})$ at ≈30°. The excess of escape probability density likely indicates a surface-hindrance effect for high-angle tumbles (also in accordance with Ref. [22]), which is not included in the model. Importantly, the same set of model parameters accounts for observations in the bulk or near a surface leading to the conclusion that, on the timescale of our observations, surfaces do not significantly modify the biochemical circuitry controlling tumbling.

From the simulated trajectories, we obtain the probability distribution $P(N_t)$ of the number of tumbles N_t needed for a swimming bacterium trapped in the surface region to finally escape (see Fig. 4) (Due to flagella bleaching, we could not obtain $P(N_t)$ from the 2C.) To understand the exponential decay behavior for $N_t \lesssim 10$, let us consider the probability p to escape out of a single tumbling event, with no memory of the previous tumbling events. Then, the probability to escape after N_t events is $P(N_t) = (1-p)^{N_t-1}p$, or $\log P(N_t) = N_t \log(1-p) + \log[p/(1-p)]$. Our data for $N_t \lesssim 10$ (Fig. 4) are consistent with $p \sim \frac{1}{3}$. Noticeably, if all tumbles reorienting a cell away from the surface would lead to a successful escape, we would rather expect $p = \frac{1}{2}$. It is as if post-tumbling reorientations for angles $< \theta_{\text{min}}$ do not lead to escapes, where $\int_{\theta_{\text{min}}}^{\pi/2} (\cos\theta/2) d\theta = \frac{1}{3}$, or $\theta_{\text{min}} = \arcsin(\frac{1}{3}) \approx 19°$, which is consistent with the extent of the "dip" in the experimental $P(\theta_{\text{out}})$ of Fig. 2(c). The symbols' colors in Fig. 4 give the mean δX, hence the "tumbling mood" when cells leave the surface region. Bluish symbols for $N_t \lesssim 10$ indicate that a majority of escaping bacteria are in a long run-time "mood" (or low δX). These bacteria are likely to escape and go far away from the surface before tumbling again. Thus, they populate the initial exponential decay. In other words, to escape, a bacterium has to tumble while being in a long-run mood. Yellowish symbols for $N_t \gtrsim 10$ show a minor population of short run-time cells for which tumble does not lead to efficient escape. Their behavior then deviates from the initial exponential decay. In both cases, bacteria will stay at surfaces for a long time but for different reasons. Numerically, for a mean run time $\langle \tau_r \rangle = 2.32$ s, we found for bacteria strictly at the surface ($\Delta z = 0$) $\langle \tau_r \rangle = 4.87$ s, for $\Delta z < \delta$, $\langle \tau_r \rangle = 3.62$ s and in the bulk, ($\Delta z > \delta$) $\langle \tau_r \rangle = 1.73$ s. Overall, surfaces act as a preferential selector for longer run times in spite of the

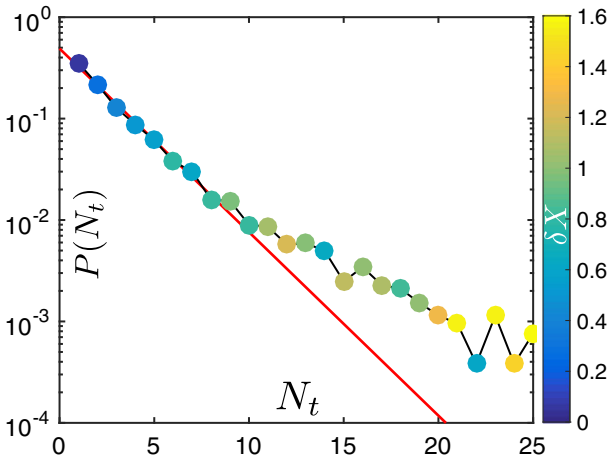

FIG. 4. Distribution of number of tumbles N_t during a stay at a surface. The red line is proportional to $P(N_t) = (1-p)^{N_t-1}p$ with $p = (1/2.9)$, which gives a mean number of tumbles of $\langle N_t \rangle^* = 2.4$, compared with $\langle N_t \rangle = 3.5$, the mean of the whole distribution. Symbol colors show the dimensionless average CheY-P concentration δX when leaving the surface.

presence of a frequently tumbling subpopulation in the surface region.

Summary and conclusions.—Using a novel 2*C*3DT method, we measured for a wild-type *E. coli*, the distributions of residence times at a solid surface, incoming and escaping angles, and tumbling times. We found that tumbling is the mechanism by which bacteria escape from surfaces. Observations are reproduced quantitatively by a model accounting for a stochasticity in the concentration of a protein (CheY-P) controlling the run-to-tumble transition rate and leading to a "behavioral variability" of run times. This indicates that the large distribution of residence times is a direct consequence of the non-Poissonian run-to-tumble statistics. The model solves a paradox where tumbling appears to be a quite efficient mean to escape from surfaces even though wild-type bacteria are likely to be trapped much longer than the typical run time. In this picture, a population of monoclonal bacteria will present a large distribution of motility features, significantly biased by the presence of surfaces. Heterogeneity in bacterial populations is usually seen as the consequence of a variety of selection pressures such as "bet hedging" against environmental change [40]. Our findings about surface residence prompt the speculation that behavioral variability in the "tumbling mood" may be a form of bet hedging against planktonic and surface living, allowing different subpopulations to optimize their behavior at every moment relative to chemotaxis in the bulk [41] and long surface residence leading to biofilm formation. Evaluating this suggestion obviously requires further research to assess precisely the role of internal noise associated with the chemotactic machinery driving the motor rotation in the context of the different possible "life styles" of *E. coli* in their natural habitats.

This work was supported by Grant No. ANR-15-CE30-0013, "BacFlow" CNRS/Royal Society Grants No. PHC-1576 and No. IE160675, and the Institut Pierre-Gilles de Gennes (Investissements d'avenir ANR-10-EQPX-34). A. L. and G. J. acknowledge support from the ERC Consolidator Grant PaDyFlow under Grant Agreement No. 682367. E. C. is supported by Institut Universitaire de France. V. A. M., J. A., A. D., and W. C. K. P. were funded by ERC (AdG 340877 PHYSAPS).

[1] M. C. Marchetti, J. F. Joanny, S. Ramaswamy, T. B. Liverpool, J. Prost, M. Rao, and R. A. Simha, Rev. Mod. Phys. **85**, 1143 (2013).
[2] H. M. López, J. Gachelin, C. Douarche, H. Auradou, and E. Clément, Phys. Rev. Lett. **115**, 028301 (2015).
[3] V. A. Martinez, E. Clment, J. Arlt, C. Douarche, A. Dawson, J. Schwarz-Linek, A. K. Creppy, V. kultty, A. N. Morozov, H. Auradou, and W. C. K. Poon, Proc. Natl. Acad. Sci. U.S.A. **117**, 2326 (2020).
[4] A. P. Petroff, X.-L. Wu, and A. Libchaber, Phys. Rev. Lett. **114**, 158102 (2015).
[5] A. P. Berke, L. Turner, H. C. Berg, and E. Lauga, Phys. Rev. Lett. **101**, 038102 (2008).
[6] G. Li and J. X. Tang, Phys. Rev. Lett. **103**, 078101 (2009).
[7] K. Drescher, J. Dunkel, L. H. Cisneros, S. Ganguly, and R. E. Goldstein, Proc. Natl. Acad. Sci. U.S.A. **108**, 10940 (2011).
[8] E. Perez Ipiña, S. Otte, R. Pontier-Bres, D. Czerucka, and F. Peruani, Nat. Phys. **15**, 610 (2019).
[9] M. P. Schultz, J. A. Bendick, E. R. Holm, and W. M. Hertel, Biofouling **27**, 87 (2011).
[10] G. D. Bixler and B. Bhushan, Phil. Trans. R. Soc. A **370**, 2381 (2012).
[11] K. Bruellhoff, J. Fiedler, M. Möller, J. Groll, and R. E. Brenner, International Journal of Artificial Organs **33**, 646 (2010).
[12] G. dong Kang and Y. Ming Cao, Water Res. **46**, 584 (2012).
[13] C. Marcato-Romain, Y. Pechaud, E. Paul, E. Girbal-Neuhauser, and V. Dossat-Ltisse, Biofouling **28**, 305 (2012).
[14] R. M. Wheatley and P. S. Poole, FEMS Microbiol. Rev. **42**, 448 (2018).
[15] O. E. Petrova and K. Sauer, J. Bacteriol. **194**, 2413 (2012).
[16] H. H. Tuson and D. B. Weibel, Soft Matter **9**, 4368 (2013).
[17] A. Creppy, E. Clément, C. Douarche, M. V. D'Angelo, and H. Auradou, Phys. Rev. Fluids **4**, 013102 (2019).
[18] N. Figueroa-Morales, A. Rivera, R. Soto, A. Lindner, E. Altshuler, and É. Clément, Sci. Adv. **6**, eaay0155 (2020).
[19] P. J. Mears, S. Koirala, C. V. Rao, I. Golding, and Y. R. Chemla, eLife **3**, e01916 (2014).
[20] L. Turner, L. Ping, M. Neubauer, and H. C. Berg, Biophys. J. **111**, 630 (2016).
[21] T. Eisenstecken, J. Hu, and R. G. Winkler, Soft Matter **12**, 8316 (2016).
[22] M. Molaei, M. Barry, R. Stocker, and J. Sheng, Phys. Rev. Lett. **113**, 068103 (2014).
[23] N. Figueroa-Morales, R. Soto, G. Junot, T. Darnige, C. Douarche, V. A. Martinez, A. Lindner, and E. Clément, Phys. Rev. X **10**, 021004 (2020).
[24] H. C. Berg, *E. coli in Motion* (Springer, New York, 2004).
[25] T. Darnige, N. Figueroa-Morales, P. Bohec, A. Lindner, and E. Clément, Rev. Sci. Instrum. **88**, 055106 (2017).
[26] J. Schwarz-Linek, J. Arlt, A. Jepson, A. Dawson, T. Vissers, D. Miroli, T. Pilizota, V. A. Martinez, and W. C. Poon, Colloids Surf. B **137**, 2 (2016).
[27] See Supplemental Material at http://link.aps.org/supplemental/10.1103/PhysRevLett.128.248101 for more details about protocols, data analysis and simulations, which includes Refs. [28–33].
[28] S. K. DeWitt and E. A. Adelberg, Genetics **47**, 577 (1962).
[29] L. Turner, A. S. Stern, and H. C. Berg, J. Bacteriol. **194**, 2437 (2012).
[30] C. Merlin, S. McAteer, and M. Masters, Tools for characterization of Escherichia coli genes of unknown function, J. Bacteriol. **184**, 4573 (2002).
[31] T. Pilizota and J. W. Shaevitz, Biophys. J. **104**, 2733 (2013).

[32] Y. Tu and G. Grinstein, Phys. Rev. Lett. **94**, 208101 (2005).
[33] J. Saragosti, P. Silberzan, and A. Buguin, PLoS One **7**, e35412 (2012).
[34] H. C. Berg and D. A. Brown, Nature (London) **239**, 500 (1972).
[35] Z. Qu, F. Z. Temel, R. Henderikx, and K. S. Breuer, Proc. Natl. Acad. Sci. U.S.A. **115**, 1707 (2018).
[36] M. Seyrich, Z. Alirezaeizanjani, C. Beta, and H. Stark, New J. Phys. **20**, 103033 (2018).
[37] E. Korobkova, T. Emonet, J. M. Vilar, T. S. Shimizu, and P. Cluzel, Nature (London) **428**, 574 (2004).
[38] E. Lauga, W. R. DiLuzio, G. M. Whitesides, and H. A. Stone, Biophys. J. **90**, 400 (2006).
[39] S. Bianchi, F. Saglimbeni, and R. Di Leonardo, Phys. Rev. X **7**, 011010 (2017).
[40] I. G. de Jong, P. Haccou, and O. P. Kuipers, BioEssays **33**, 215 (2011).
[41] S. Dev and S. Chatterjee, Phys. Rev. E **97**, 032420 (2018).